Visual Appearance of Surface Distress in PCC Pavements: II. Crack Modeling

NORMAN WITTELS AND TAHAR EL-KORCHI

In the previous paper in this Record, the fundamental engineering data required to design automated pavement surface distress evaluation systems were discussed; in particular, luminance values along the crack sidewalls and bottom were used to calculate the visual contrast between the crack and surrounding pavement. Image contrast is an important parameter in machine vision design. Computer modeling of light reflection in portland cement concrete (PCC) pavement cracks can be used to simulate the luminance values in pavement images. Such a model, presented for the luminance of long rectangular slots in homogeneous pavements, is experimentally validated, extended, and applied to pavement surface distress. The model and resulting data are useful for the design of image acquisition and image processing systems and in the simulation of worst case images for testing pavement evaluation systems.

Automated pavement surface distress evaluation systems are an important ingredient in the computerized pavement management systems (PMS) being constructed by many transportation agencies. Although a number of experimental and developmental evaluation systems have been built, they have not demonstrated a consistently high degree of reliability in use. In the previous paper in this Record, the technical challenges associated with building reliable pavement inspection systems were examined and a detailed understanding of the luminance values along the sidewalls and bottoms of cracks was shown to help design image acquisition and image processing systems. Although it is easy to measure the crack luminance values for any given crack and lighting arrangement, it is difficult to predict the luminance values. Without some way to make such predictions, one cannot easily select worst case images for testing systems, nor can one gain the understanding that aids in system design. Computer simulations of cracks in portland cement concrete (PCC) pavements can be used for making such predictions and simulation results can be used for designing automated pavement inspection systems.

SIMULATION

There are three steps in developing a satisfactory computer simulation of crack luminance values: producing a mathematical model of a crack, validating the model by comparing simulated with actual luminance values, and showing how to apply the model to problems of automated pavement inspection. These steps will be discussed in that order.

N. Wittels, Electrical Engineering Department, T. El-Korchi, Civil Engineering Department, Worcester Polytechnic Institute, Worcester, Mass. 01609.

Simulation Model

There are many possible physical models of pavement distress from which to build a mathematical model of crack luminance values. The simplest is to assume that the pavement is a homogeneous material and that a crack is a straight rectangular slot in the pavement. The later section on interreflection calculation contains a detailed description of the model and its implementation. Because this model is a gross oversimplification of real pavements and real pavement surface distress, it is first shown that the model accurately simulates the appearance of rectangular slots in homogeneous pavements. In the following discussion, the results from the simple model are related to characterization of actual pavement distress.

The key physical parameters of the model are the material reflectivities, the ratio of directed to ambient illumination, the incidence direction of the directed illumination, and the crack geometry. The ranges of possible values for most of these parameters are bounded; the applicable values are discussed in the following paragraphs.

In the previous paper in this Record, reflectivity values were measured on typical PCC pavement materials. Mortar has a reflectivity of 0.30 to 0.35 for both freshly prepared surfaces and for cut or fractured surfaces, implying that between 30 and 35 percent of all of the incident light is diffusely reflected back from its surface. The surface reflectivity of old pavements is about half as large. Aggregate materials have reflectivities between 0.05 and 0.90; the most commonly used materials have reflectivities between 0.15 and 0.60. At most one of the crack sidewalls or the crack bottom can be a piece of aggregate. In summary, the pavement surface has a reflectivity of roughly 0.15, two of the crack surfaces have reflectivity about 0.30, and the third crack surface has reflectivity between 0.15 and 0.60, depending on the aggregate material.

There are two types of lighting used in automated pavement surface distress evaluation, natural and artificial. Natural lighting is a mixture of skylight and sunlight (*1*,*2*). Skylight is omnidirectional or ambient lighting and is assumed to arrive with equal intensity from the entire hemisphere of sky. An artificial lighting system that surrounds the pavement with omnidirectional lighting (*3*) can be considered to be skylight. The inside surfaces of cracks illuminated by skylight receive somewhat less illuminance than the pavement surface because less of the sky is seen (the sidewalls occlude part of the hemisphere of illumination). Sunlight can be considered to be perfectly collimated light (as from a distant point source) because the shadow unsharpness in a crack image caused by the sun's finite size is much smaller than the resolution limit of an automated pavement evaluation system. Spotlight illumination can be

modeled in the same way as sunlight but artificial illumination using multiple sources or extended sources may require modifications to the model, as discussed in a later section. Absolute object luminances are not usually used in machine vision because the best system operation requires that the camera aperture (or illumination intensity) be adjusted to place the sensor illuminance in the most luminous portion of the scene just below the camera's saturation level (*4*). Therefore, only the ratio of the components of surface illuminance caused by skylight and sunlight is important in the calculation. The skylight-sunlight ratio can have values between 1:0 (a totally overcast day) and 1:8 (noon on a bright sunlit day) or 0:1 (a spotlight at night with no other indirect illumination). With artificial illumination, this system can be designed to produce almost any value of this ratio.

Skylight is omnidirectional, but sunlight has a definite direction of incidence. Two angles are required to specify the sunlight direction. The polar angle (angle from the zenith) can have values between a low value of approximately the local latitude minus 23° (the minimum is 0° for those latitudes where the sun passes through zenith) to 90° (horizon), although angles greater than about 70°—corresponding to the sun low on the horizon—overly emphasize the pavement surface texture and are usually inappropriate for surface distress evaluation. The azimuthal angle can have any value between 0° (perpendicular to the crack sidewall) and 90° (directed along the crack).

For purposes of the simple model, crack geometry is specified by a width and a depth. In general, other information about the local crookedness of the crack may also be important in determining its luminance values. In the later section on interreflection, two physical dimensions are used in the model, crack depth and width. However, because dimensionless distances are used in the model there is only one independent variable, the ratio of crack depth to width. Wide, shallow cracks have depth-width ratios less than 1 and deep cracks have ratios greater than 1.

Using the parameters summarized, it is straightforward to calculate the sidewall, crack bottom, and pavement surface luminances for the simplified crack. Before applying the results it is appropriate to validate the model.

Model Validation

To validate the model, the luminances of pavements that matched the simple geometry were measured. Mortar samples were prepared using uniform quartz sand and portland cement with a 3:1 weight proportion and a water-cement ratio of 0.3. The samples were cured for 3 days and rectangular slots were cut with depth-width ratios between 0.4 and 4.0 (Figure 1, top). The slots were illuminated with mixtures of ambient and directed lighting and were observed perpendicular to the surface (the preferred observation direction for an automated inspection system because it minimizes the perspective distortion of the imaging optics and maintains constant resolution across the image). Illumination was provided by 3,200°K quartz halogen lamps. Color temperature correction was not required because the color of the samples is neutral. The directed illumination was provided by a collimating optical system to simulate sunlight, and the ambient illumination was produced by surrounding the sample with a cone of translucent material uniformly illuminated by multiple light sources (Figure 1, bottom). Illumination uniformity was verified using the method proposed by Goodman (*5*). Digital images were made with a Schneider 50-mm Companon-S lens and a CIDTEC 2505A solid-state camera whose output was sampled by a Data Translation DT2851 frame grabber. The camera output voltage levels were converted to sensor illuminances (*6–8*), which are proportional to crack luminances. The measured luminances along the bottom of the slots were compared with the surface luminances.

There are two ways to compare measured with calculated luminance values: they can either be compared directly, pixel by pixel, or average values can be compared. Figure 2 shows a direct comparison of simulated and measured luminances for a representative slot. In this case, the ratio of direct to indirect illumination was 1:1 and the direct illumination was incident at the angles $\Phi = 45$ degrees, $\Theta = 0$ degrees, where the angles are defined in Figure 6. The values have been normalized to the average pavement surface luminance. The ripple in the measured data is an inherent part of the electronic signal and has a typical peak-to-peak value of about 5 percent of the maximum signal level. The measured and simulated values agree well, within about 10 percent at all locations within the crack. The unsharpness of the measured values at the crack edges is inherent in solid state video cameras (*6,7*). Other cases tested produce comparable agreement.

Although direct pixel-by-pixel comparison between simulated and actual luminance values across the slot is an important step in validating the model, detailed luminance values are not the most useful measure of image contrast for automated inspection system design. The large field of view of an automated pavement evaluation system, up to a 12-ft (3.6-m) highway lane width, and the relatively poor resolution limits of machine vision cameras, typically less than 1/500 of the field of view, result in digital images in which small cracks, the hardest to see, are rarely more than one or two pixels wide. A camera's output is a measure of the average image illuminance across each pixel, so a better measure of image contrast is the average luminance value along the bottom of the crack (or the imaged sidewall, if the crack is observed obliquely). Figure 3 shows measured and calculated average bottom luminances, normalized to the pavement surface luminance, for several representative slot geometries and two lighting conditions. The values agree well, to within $\pm(5–10)$ percent of maximum value, for cracks with depth-width ratios in the range 0.8 to 2.0. For smaller ratios (wide, shallow cracks), the samples were too narrow so the luminances were higher than predicted by the model, which assumes that slots are infinitely long. For higher ratios (thin, deep cracks), the luminances were too low to be measured accurately by the experimental arrangement used. In the one measurement where a spot photometer was substituted for the video camera, the bottom luminance agreed with the predicted value. The tests have not been exhaustive but they give a preliminary indication that the model provides accurate simulations of the luminance of rectangular slots in portland cement mortar samples. Further testing of the model is planned and will be reported in later publications. In the next section, the applicability of this model to digital images of pavement distress is discussed.

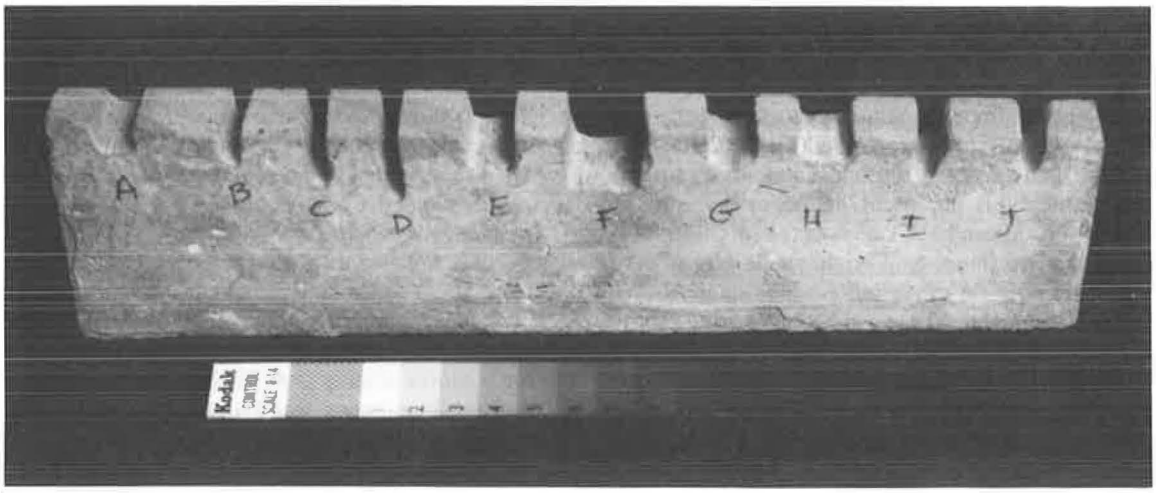

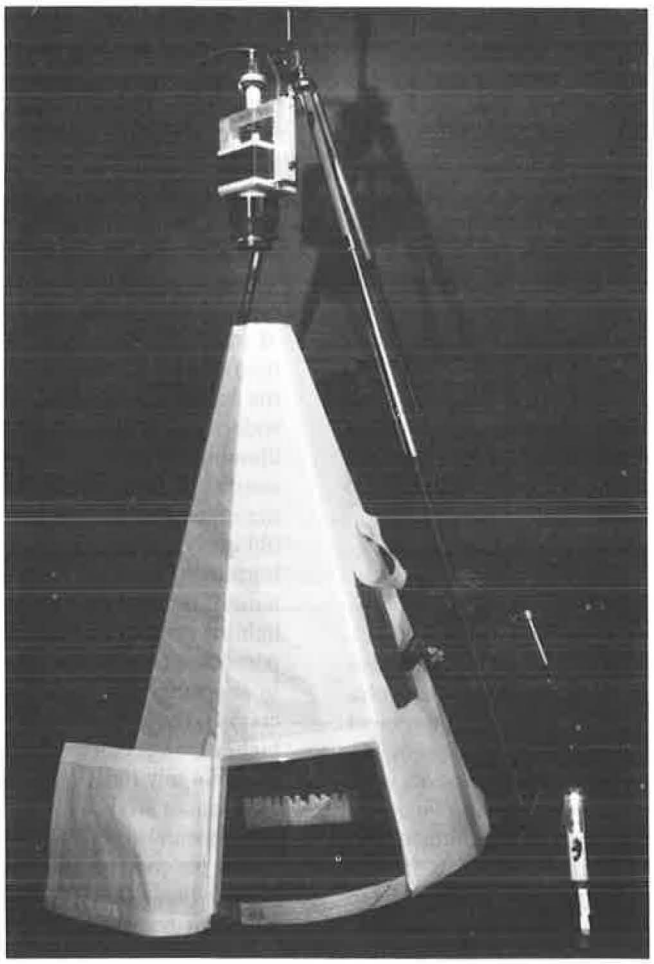

FIGURE 1 Photographs of the simulation validation experiment: top, portland cement mortar sample showing cut rectangular slots of varying depths and widths; bottom, experimental arrangement showing sample, lighting, and camera.

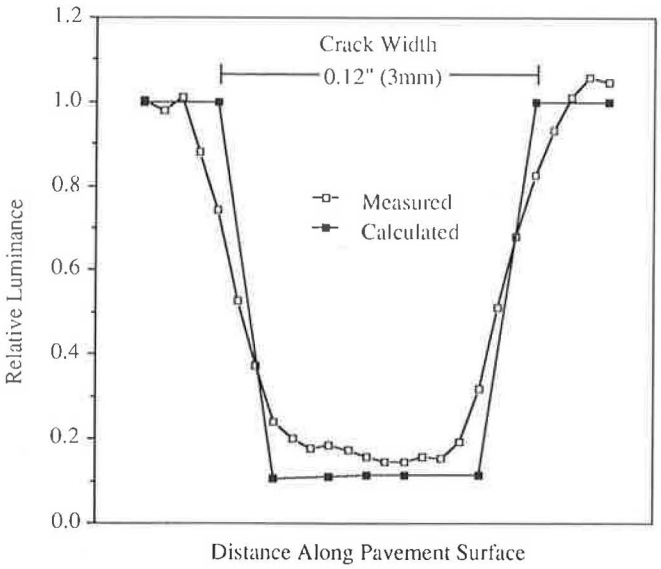

FIGURE 2 Comparison of crack luminances simulated by a computer and measured using a 0.12-in. (3-mm) wide and 0.20-in. (5-mm) deep slot cut in a prepared mortar sample.

DISCUSSION

In this section, the limitations of the simple luminance simulation model when used to characterize pavement distress are discussed. Also, future work that leads toward a complete characterization of the visual appearance of pavement surface distress is outlined.

Limitations of the Model

There are two concerns about using the simulation model to simulate PCC pavement surface distress: pavement cracks are not rectangular slots and PCC pavements are not homogeneous because they contain aggregate in addition to mortar. In this subsection, these concerns are discussed.

The first model limitation concerns crack geometry: cracks are generally neither straight nor perpendicular to the pavement surface, nor are their depths and widths constant along their lengths. The model, which is a two-dimensional interreflection model, does not allow geometry changes along the crack length. From three-dimensional extensions of this model, calculations show that light reflected from a region on a crack sidewall or bottom can only significantly affect the luminances of other crack regions that lie within a few crack widths distance. Thus, except for small (distances less than the crack width) transition regions where abrupt geometric changes occur, the crack can be modeled as line segments along which the model is valid. The crack illuminance is relatively insensitive to small changes in illumination angle; to first order, it varies as the cosine of the angle at which the light strikes the illuminated surfaces. Thus, straight line segments can be used to model most crack geometries. More work needs to be done to characterize the crack luminance in the transition regions.

In order to test the statement that a straight line model can be applied to pavement distress, a sample was prepared using the same mortar as the samples for the model validation pre-

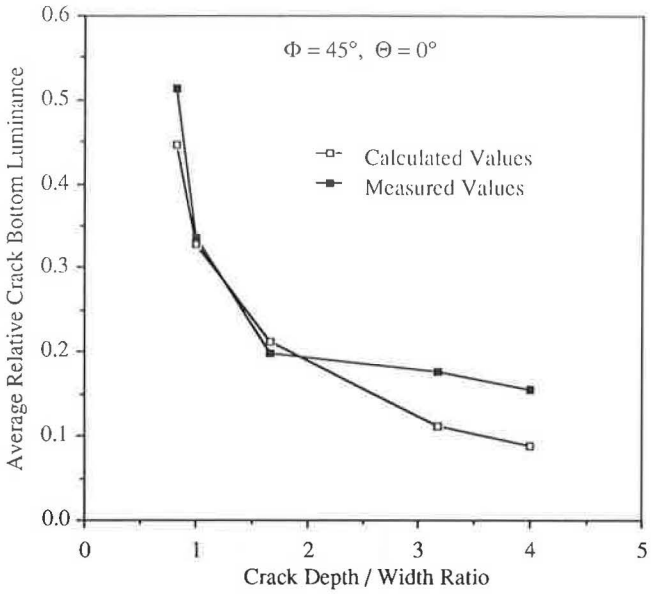

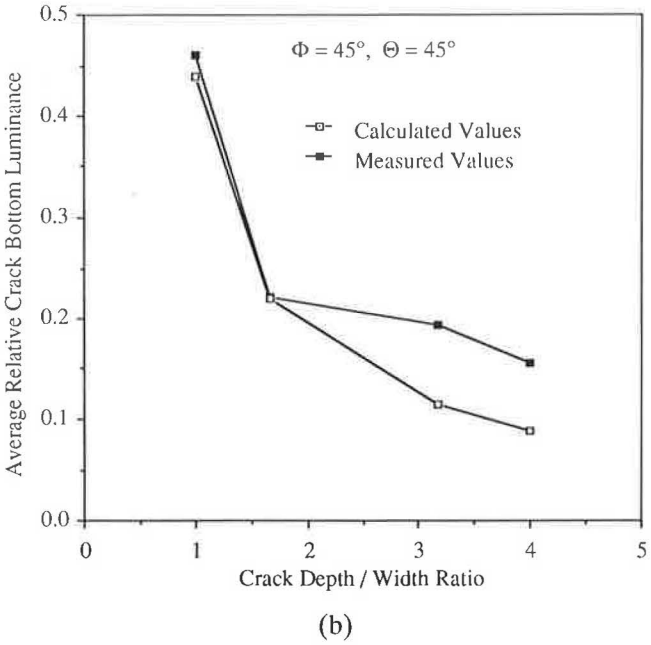

FIGURE 3 Comparison of simulated and measured average crack bottom luminances, normalized to the average pavement surface luminance, for cracks with several depth/width ratios (a) for illumination conditions as in Figure 2, Φ = 0 degrees and (b) for illumination conditions as in Figure 2, Θ = 45 degrees.

viously. It was cracked and mounted on a mechanical slide to make the crack width adjustable; the same configuration but with a different sample was shown in Figure 7 of El-Korchi and Wittels (*1*). The average crack bottom luminance was measured for several illumination conditions and crack widths. The bottom values were typically within ±(5–10) percent of the average value. Most of that variation is attributable to noise in the image acquisition system. Only a few tests were performed, but no major variations in bottom luminance were

found, so it is reasonably certain that a straight slot model is useful for understanding and simulating the luminance of cracks in distressed portland cement mortar samples.

The second limitation concerns reflectivity changes. In an image of a PCC pavement, the luminances of the mortar and aggregate are proportional to their respective reflectivities; visible contrast is caused by reflectivity differences between coarse aggregate and mortar. As pointed out earlier, the crack surfaces will all have the reflectivity of mortar except for at most one of the sidewalls or the bottom, which will have the reflectivity of aggregate. In the simulation model, the reflectivities of the crack surface, sidewalls, and bottom can be specified independently, allowing representation of all of the crack cases although it does not account for reflectivity changes along the crack length.

Unlike the effects of geometric changes just discussed, reflectivity changes are abrupt at the aggregate-mortar boundaries. Because material reflectivity difference is a major cause of image contrast, understanding the exact luminance values in these boundary regions is important in specifying and evaluating image processing algorithms that distinguish distressed from sound pavement. The simple model can simulate crack contrast in the region adjacent to a piece of aggregate but it cannot give detailed information about how the contrast varies at the aggregate boundaries. Figure 8 in El-Korchi and Wittels, the previous paper in this Record, shows digital images of a 0.06-in. (1.5-mm) crack in a prepared PCC sample containing hand-selected course granite aggregate with a maximum size of ⅜ in. (10 mm). The most luminous portion of Figure 8b in El-Korchi and Wittels is a shelf of mortar-covered aggregate about 1/16 in. (1.5 mm) below the pavement surface. The measured luminance on the shelf, relative to the average surface luminance, is 1.08, and the luminance calculated for a rectangular slot with the same dimensions and reflectivities is 1.02; the agreement between the modeled and measured luminance values is about at the limit of the experimental errors. The calculation provides luminance values when the crack bottom is mortar or when it is aggregate, but does not provide detailed information about how the luminance varies between them in the transition region at the ends of the aggregate. Enhancements to the model may provide a tool for future studies of the image contrast in these transition regions.

Total Characterization of the Pavement Images

In this section, limitations of the simulation model have been discussed, and simple arguments and measurements have been used to show that the model can be applied to understanding surface distress in PCC pavements. More testing and analysis need to be done to determine whether the model can be applied universally. That work is in progress and will be reported later. On the assumption that the model, or some modification of it, can be applied to most pavement conditions, it is useful to speculate on future directions that the work can take. First, the model can be applied to the problem of designing image acquisition and illumination systems. For example, an exhaustive search of crack contrasts calculated for a wide range of illuminating conditions may provide insights in how to optimize the illumination for crack detection. Or, calculated crack contrast can be used to write the video noise specification that will enable the image acquisition equipment to meet the system specification regarding probability of crack detection.

The second major use for computer models of pavement distress is in aiding development and testing of image processing algorithms. The pavement image contains signals from cracks and from aggregate on the concrete surface. In this paper, the visual appearance of cracks was described; comparable work remains to characterize the visual appearance of aggregate. Also, only PCC pavements were discussed; extension of the modeling to include surface distress in overlays and asphaltic concretes would be useful.

INTERREFLECTION CALCULATION

This section contains detailed information about the interreflection calculation model. It is presented for the benefit of those requiring detailed knowledge of the methods but it is placed at the end of the paper so as not to impede the reader who does not need this level of detail. Note that photometric units for light are used throughout this work. Originally designed to measure the response of the human eye to broadband natural illumination (sunlight), they are well suited to working with solid state cameras whose sensors are spectrally matched to the sensitivity of the human eye.

Cracks are jagged, irregular gaps in the pavement. For modeling purposes, they are considered to be rectangular slots of infinite length. The key parameters in the model are shown in Figure 4. Ambient lighting is omnidirectional and represents skylight; it is characterized by its apparent luminance. Directed lighting represents sunlight or the illumination from a spotlight directed at the pavement; it is characterized by an illuminance and a direction. The surfaces are assumed to be diffuse reflectors with four distinct reflectivities: pavement surface, crack sidewalls (the sides lit and unlit by the directed illumination), and crack bottom.

The crack is illuminated by one of two sources, ambient or direct illumination, as shown in Figure 5. In the model for ambient illumination (left), a uniformly diffuse emitter with luminance L_0 covers the top of the crack. In the model for directed illumination (right), a perfectly collimated beam with illuminance E_0 illuminates all surfaces except where shadowed by crack edges. The total illuminance at each point is the sum of two components. Using the incidence angles shown in Figure 6 (Φ is the polar angle relative to the pavement surface normal and Θ is the azimuthal angle relative to the crack sidewall normal), the illuminances at a point P_1 on the sidewall and a point P_2 on the crack bottom due to directed illumination are given by

$$E_{1,D} = E_0 \sin \Phi \cos \Theta$$

$$E_{2,D} = E_0 \cos \Phi \tag{1}$$

Note that the direct illuminance equations only apply to those portions of the crack walls and floor that are not shadowed by the crack edge. The shadow edge falls either on the crack bottom at $x = D \tan \Phi \cos \Theta$ or on the crack sidewall at $z = W/(\tan \Phi \cos \Theta)$, where the coordinate axes and dimensions are shown in Figure 5. The illuminances of the

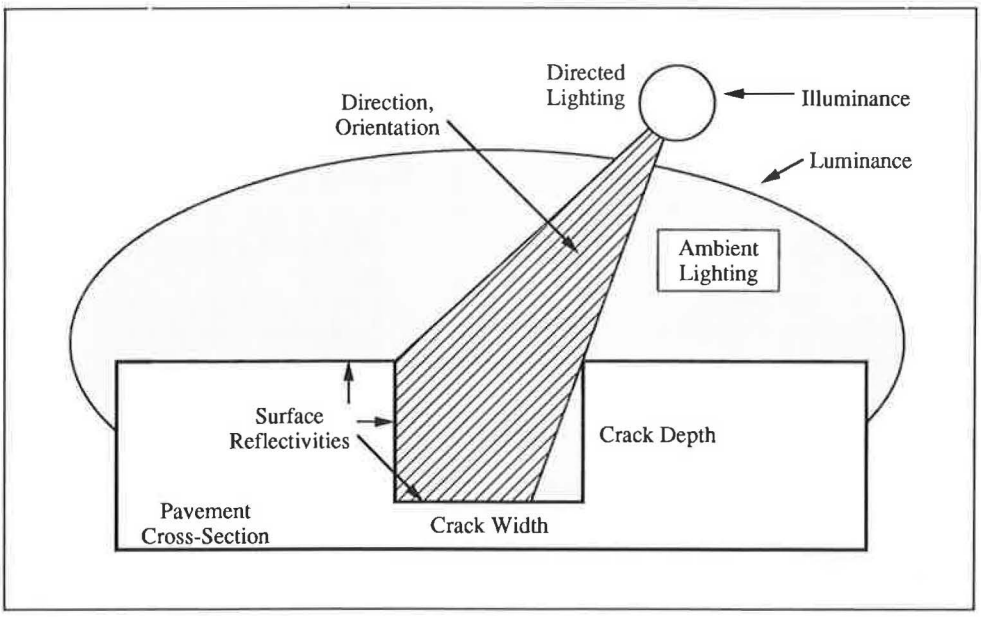

FIGURE 4 Cross-sectional view of an ideal pavement crack showing the adjustable parameters in the mathematical model.

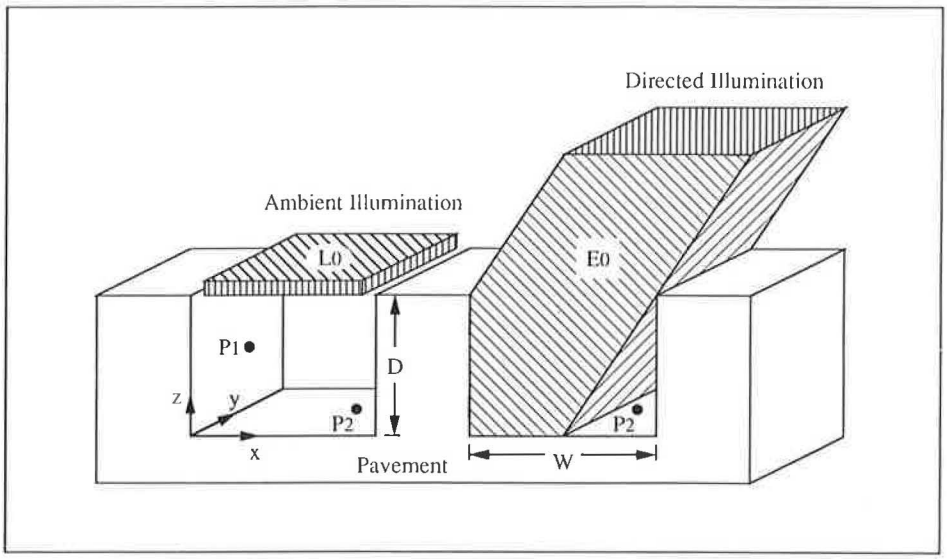

FIGURE 5 Thin slice through an infinitely long ideal crack showing definitions of the coordinate system, the symbols used for crack width and depth, and ideal illumination models for ambient illumination (left) and directed illumination (right).

same two points due to ambient illumination are given by the following equations:

$$E_{1,A} = \frac{\pi L_0}{2}\left(1 - \frac{z}{\sqrt{z^2 + W^2}}\right)$$

$$E_{2,A} = \frac{\pi L_0}{2}\left(\frac{x}{\sqrt{x^2 + D^2}} + \frac{(W - x)}{\sqrt{(W - x)^2 + D^2}}\right) \quad (2)$$

The total incident illuminance is the sum of two terms:

$$E_1 = E_{1,A} + E_{1,D};\ E_2 = E_{2,A} + E_{2,D}$$

A portion of the incident light is reflected back into the camera and on to all surrounding surfaces, including other parts of the crack. This interreflection between crack surfaces can significantly alter the apparent crack luminances and must be included in the calculation.

Divide the surface inside the crack into N infinitely long strips as shown in Figure 6, and assume that all surfaces reflect diffusely and that the reflectivities are as defined. If the total (incident plus interreflected) illuminance falling on the ith strip is E_i then the luminance of that strip is $L_i = R_i E_i/\pi$, where R_i is the strip's reflectance. In addition to the direct and ambient incident illuminances, there is a contri-

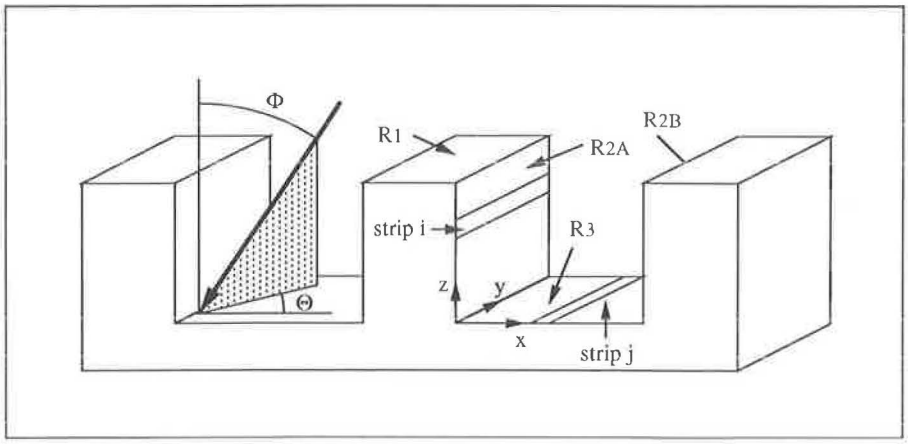

FIGURE 6 Polar coordinates used to define orientation of direct illumination (left) and two interreflecting strips (right).

bution from the light reflected by each of the other strips (except those lying on the same crack face as the ith strip). The contribution to E_i caused by L_j is

$$E_i = \frac{\pi L_j}{2}\left(\frac{z}{\sqrt{x_{jL}^2 + z^2}} - \frac{z}{\sqrt{x_{jR}^2 + z^2}}\right) = A_{ij}E_j \tag{3}$$

where x_{jL} is the left edge of the jth strip and x_{jL} is the right edge. This equation applies for the case illustrated—i is on a sidewall and j is on the crack bottom. Similar expressions apply to the other cases. The illuminances are thus related by a set of N linear equations:

$$E_i - \sum_{j \neq i}^{N} A_{ij}E_j = E_{i,D} + E_{i,A} \tag{4}$$

These equations are solved simultaneously to calculate the illuminance, and hence the luminance values, of each strip. If a further goal is to simulate the visual appearance of the crack, it can be calculated from the luminance values by using the perspective transformation techniques of computer graphics (*9*,*10*).

Note, the two-source model is satisfactory for simulating cracks illuminated by all possible combinations of skylight and sunlight. Because artificial illumination systems can be designed to produce arbitrary spatial and angular illuminance variations, this model may require modification. The right side of the last set of equations would be replaced by the strip illuminances caused by the light sources. The method of solution will otherwise remain the same as that discussed previously.

ACKNOWLEDGMENTS

The authors gratefully acknowledge the help and encouragement of many people who contributed to this work. Their colleagues M. Ward and M. Gennert aided in developing the technical strategy and some of the analyses used in the work. M. Turo of the Massachusetts Department of Public Works helped them understand the operational and technical requirements of automated pavement evaluation systems. J. Sage of the WPI CE Department aided in selecting the aggregate materials used. B. Bian contributed ideas on interreflection calculation methods. A. Bielund, S. Annecharico, and J. LeBlanc assisted in the calculations and experiments. This work was supported by the Research Development Council of the Worcester Polytechnic Institute.

REFERENCES

1. J. E. Kaufman (ed.). *IES Lighting Handbook*. Illuminating Engineering Society of North America, New York, 1981.
2. W. Thomas, Jr. (ed.). *SPSE Handbook of Photographic Science and Engineering*. John Wiley, New York, 1973.
3. J. Baker, B. Dahlstrom, K. Longenecker, and T. Buu. Video Image Distress Analysis Technique for Idaho Transportation Department Pavement Management System. In *Transportation Research Record 1117*, TRB, National Research Council, Washington, D.C., 1987, pp. 159–163.
4. N. Wittels and S. H. Zisk. Lighting Design for Industrial Machine Vision. *Proc., Society of Photooptical Instrumentation Engineers*, Vol. 728, 1986, pp. 47–56.
5. D. S. Goodman. Illumination Analysis with a Reflecting Sphere. *Applied Optics*, Vol. 24, 1985, pp. 1217–1219.
6. J. R. McClellan. Characterization and Correction of Image Acquisition System Response for Machine Vision. Master's thesis, Worcester Polytechnic Institute, Worcester, Mass., 1989.
7. J. R. McClellan et al. Characterization and Correction of Image Acquisition System Response for Machine Vision. *Proc., Society of Photooptical Instrumentation Engineers*, Vol. 1194, 1989.
8. N. Wittels et al. Lighting Design for Industrial Machine Vision. *Proc., Society of Photooptical Instrumentation Engineers*, Vol. 1005, 1988, pp. 47–56.
9. R. M. Haralick. Using Perspective Transformations in Scene Analysis. *Computer Graphics and Image Processing*, Vol. 13, 1980, pp. 191–221.
10. L. G. Roberts. Homogeneous Matrix Representation and Manipulation of *N*-Dimensional Constructs. Report MS-1405, MIT Lincoln Laboratory, Cambridge, Mass., 1966.

Publication of this paper sponsored by Committee on Pavement Monitoring, Evaluation, and Data Storage.